A Letters Journal Exploring the Frontiers of Physics

March 2008

EPL, **81** (2008) 64004
doi: 10.1209/0295-5075/81/64004

www.epljournal.org

Conservation of energy in coherent backscattering of light

S. Fiebig[1], C. M. Aegerter[1], W. Bührer[1], M. Störzer[1], E. Akkermans[2], G. Montambaux[3] and G. Maret[1]

[1] *Fachbereich Physik, University of Konstanz - Box M621, 78457 Konstanz, Germany*
[2] *Department of Physics, Technion Israel Institute of Technology - 32000 Haifa, Israel*
[3] *Laboratoire de Physique des Solides, CNRS UMR 8502, Université Paris-Sud - 91405 Orsay, France*

received 8 November 2007; accepted in final form 26 January 2008
published online 22 February 2008

PACS 42.25.Dd – Wave propagation in random media
PACS 73.20.Fz – Weak or Anderson localization
PACS 42.25.Hz – Interference

Abstract – Although conservation of energy is fundamental in physics, its principles seem to be violated in the field of wave propagation in turbid media by the energy enhancement of the coherent backscattering cone. In this letter we present experimental data which show that the energy enhancement of the cone is balanced by an energy cutback at all scattering angles. Moreover, we give a theoretical description which is in good agreement with these data. The additional terms needed to enforce energy conservation in this description result from an interference effect between incident and multiply scattered waves, which is reminiscent of the optical theorem in single scattering.

Introduction. – Conservation of energy is one of the most fundamental principles in physics, which so far has not been violated. There are however instances, where this seems to be the case at first glance. One such example is the coherent backscattering cone which appears when waves propagate in turbid media. In that case, a twofold enhancement of the backscattered intensity with respect to the diffusely scattered background is observed. This enhancement decays over an angular scale of $(kl^*)^{-1}$, where k is the wave number of the wave and l^* is the transport mean free path of the medium [1]. Due to its fundamental nature, the coherent backscattering cone can be observed with many different types of waves, such as electrons in metals [2], visible light in the laboratory [3–5] as well as in space [6], microwaves [7], seismic waves [8], and sound waves [9].

The origin of the backscattering enhancement lies in the interference of waves propagating along reciprocal paths. This interference can only spatially re-distribute the backscattered energy. Thus the energy enhancement at small angles should be accompanied by a corresponding energy cutback to ensure conservation of energy. This is because energy is conserved in Maxwell's equations, which microscopically describe the problem. However, in typical experiments, at least 10^{10} scatterers should be treated. For such large numbers of randomly distributed scattering particles a solution of Maxwell's equations is technically impossible. Therefore a collective description of the effect [1,10,11] needs to be done, where conservation of energy does not appear. Moreover, such an energy cutback has not been observed experimentally up to now. This implies that both the theoretical description as well as the experiments should be improved in order to restore conservation of energy.

Furthermore, the additional energy contribution of the coherent backscattering cone to the intensity cannot be explained by a corresponding reduction in transmission at surfaces not considered in the experiment. Rather, the backscattering cone is also observed from samples which can theoretically as well as experimentally be treated as filling an infinite half-space, meaning that the waves can reach no other surface than the one considered [1]. In addition, the energy in the cone cannot be obtained from another polarization channel, since no reduction in backscattering is observed in other polarization channels [12]. In the diffusion approximation, which is valid for the optically thick samples we will consider, a backscattering cone is only present in the polarization conserving channel, while the polarization breaking channel shows only the incoherent background of backscattering. This holds for all incoming polarizations [12]. Therefore, one can describe the problem as a scalar scattering problem where only the polarization conserving channel is considered.

The fact that a possible energy cutback is not included in any theoretical description of the backscattering cone can be problematic as the scaling of its width with kl^* is commonly used to characterize multiple scattering materials. In particular in turbid samples, when the cone becomes very broad, there has to be a sizeable correction if conservation of energy is to hold. This is for example of great importance in the study of Anderson localization of light [13], where a reliable knowledge of the parameter kl^* is needed to characterize the phase transition from diffusive transport to a localizing state [14,15].

In this letter, we present measurements of coherent backscattering, where the incoherent background is determined on an absolute scale. This is in contrast to previous investigations, where the incoherent background was determined from the wings of the backscattering data [16]. With this we are able to show that there is a reduction in backscattering intensity at all angles compensating for the enhancement in the back direction. A theoretical description which fits these data shows that the reduction in enhancement results from a new interference effect between the incident and multiply scattered waves. This is analogous to the shadow term, which accounts for flux conservation in the optical theorem [17]. In the context of weak localization, this was already discussed by Dmitriev *et al.* [18], who have calculated the scattering cross-section of multiply scattered electrons. This calculation involved a crossing similar to the one introduced here and leads to a conservation of the elastic-scattering cross-section. In multiple scattering, the terms needed to ensure energy conservation correspond to the so-called Hikami box or quantum crossing [19,20]. The present experiment constitutes a direct observation of such a scattering process, which can be described by a Hikami box playing a central role in quantum mesoscopic physics [20].

Experimental setup. – Our main setup to study the angular distribution of the backscattered light consists of 256 photosensitive diodes attached to a semi-circular arc with a diameter of 1.2 m. In its center the sample is located, facing the illuminating laser beam which is focussed through a small hole in the arc between the two central diodes [21]. To average over random speckle patterns, the sample is rotated. In this way, we can detect light over a range of $-60° < \theta < 85°$ with a resolution of $0.14°$ for $|\theta| < 10°$, $\sim 1°$ for $10° < |\theta| < 60°$ and $\sim 3°$ for $\theta > 60°$. For the illumination a continuous wave dye laser with a wavelength of 590 nm is used. The measurements are done using circularly polarized light in order to reduce the influence of single scattering. Using a mirror, we have checked that this suppression exceeds 95%, such that enhancements of 0.95 are possible with this setup. As the very tip of the cone at $\theta \simeq 0$ cannot be resolved with this setup, the central part of the backscattering cone, $|\theta| < 3°$, is measured separately using a beam splitter and a charge-coupled device (CCD) camera to a resolution of $0.01°$ [21].

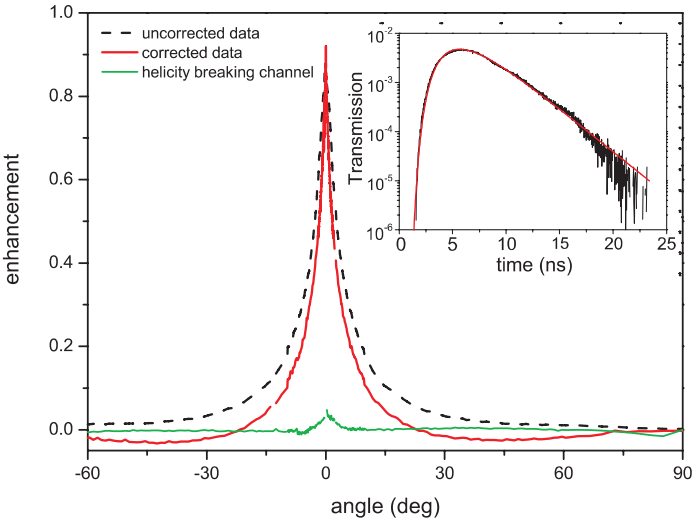

Fig. 1: (Colour on-line) Backscattering cone of R700 evaluated ignoring (dashed curve) and taking into account (full red curve) absorption in the reference sample. The former is positive for all angles, resulting in an uncompensated energy enhancement of the cone. For the latter, energy enhancement and energy cutback are balanced. This is quantified by the half-space integral of the intensity $I = -0.005(7)$. The corrected helicity breaking channel is also shown, which is very flat over the whole angular range except at the center, where a small cone is present due to imperfect polarization selection. This shows that the correction procedure works to the accuracy of 0.005, which is necessary to observe the reduction of backscattering compensating the energy in the cone. The inset shows a time-of-flight measurement of the teflon reference, which follows diffusion theory with an absorption time of 3.3 ns.

To be able to determine the intensity of the backscattered cone on an absolute scale, the incoherent background needs to be known. The intensity in the cone scales as $1/(kl^*)^2$, such that for typical values of $kl^* \simeq 10$, an accuracy of 1% is necessary to resolve the energy cutback. Note that we are able to achieve this level in spite of the fact that only 95% of singly scattered light is suppressed, since single scattering will be of the same order in the sample and the reference. As a reference sample, we have used a block of teflon. Teflon has a transport mean free path of $\simeq 300\,\mu$m and hence the backscattering cone of teflon at a wavelength of 590 nm has a FWHM of about $0.02°$. Thus the cone of teflon cannot be resolved in the wide-angle setup, and the teflon reference measurements can be considered to describe the diffuse background of the TiO_2 samples. This is also true at wide angles as any corrections due to conservation of energy would be at the level of below a ppm, which is far beyond the experimental resolution. The angle dependence is thus given by $\mu(\gamma + \mu/(\mu+1))$ when properly normalized [20]. Here $\mu = \cos\theta$ and γ is a universal parameter ($\gamma = 2/3$ in the diffusion approximation), which describes the distance over which the intensity enters the sample before being scattered. From the helicity breaking channel shown in fig. 1, it can be seen that the diffusion approximation

is valid for our experiments, since the background is completely flat at higher angles. The small cone, which is visible in the figure is due an incomplete extinction of the polarization, which leads to a cone with an enhancement of ~ 0.04. Due to the presence of this cone it is not feasible to directly use the helicity breaking data as a background, and the signal from the teflon sample has to be used instead. In treating the teflon measurement as the diffuse background, one however neglects the different albedo of teflon with respect to the sample giving a different magnitude to the background. The proper background for the sample, $\alpha_{\mathrm{inc,samp}}$, is therefore given by that of the reference, $\alpha_{\mathrm{inc,ref}}$, multiplied by the ratio of the albedos of sample and reference, $A_{\mathrm{samp}}/A_{\mathrm{ref}}$.

For an estimation of the albedos to a level of better than 1%, one needs to take into account losses at the sample/reference boundaries, as well as losses due to absorption. As we will see below, the losses due to absorption and finite thickness are both of the order of 5% for the teflon reference. Therefore already a rough estimate of the loss factors would be able to give an accuracy below 1%. Up to now however, these losses have not been fully taken into account in the evaluation of the backscattering cones [16,21].

The loss due to leakage will be of the order of the transmission through a sample, *i.e.* $l^*/L + l^*/R$, where L and R are the thickness and radius of the sample, respectively. Here, the mean free path of sample and reference can be estimated by the uncorrected cone. A quantitative estimate of the correction can be obtained by comparing the diffuse energy in an infinite half-space with the amount of energy that is left in a volume-cutout of the infinite half-space corresponding to the size of the sample/reference [11]. This will neglect edge effects, but these will be of the order of $(l^*/L)^2$, *i.e.* below the desired level. The loss factor for absorption can be calculated from the integral over the path length distribution $P(D,\tau,t)$, where D is the diffusion coefficient and τ is the absorption time. This leads to an exponential suppression of the albedo with the absorption length $L_a = \sqrt{D\tau}$. Taking both contributions together, we obtain for the albedo

$$A = e^{-\frac{2\gamma l^*}{L_a}}\left(1 - \frac{2}{\pi}\left(\arctan\left(\frac{2\gamma l^*}{L}\right) + \arctan\left(\frac{L}{R}\right)\frac{2\gamma l^*}{R}\right)\right). \tag{1}$$

Both quantities needed to calculate the albedo, D and τ, can be determined with a time resolved transmission experiment [15,22]. The time-of-flight measurements like the data from the teflon reference shown in the inset of fig. 1 directly give the path length distribution inside the sample, which is a function of D and τ only. In our experiment, the same dye laser is used as in the backscattering experiments, thus making a possible wavelength dependence of D and τ irrelevant. Given the low absorption and high optical thickness of our usual samples, they typically have albedos in excess of 0.995, such that only the losses of the teflon reference are important, for which we obtain

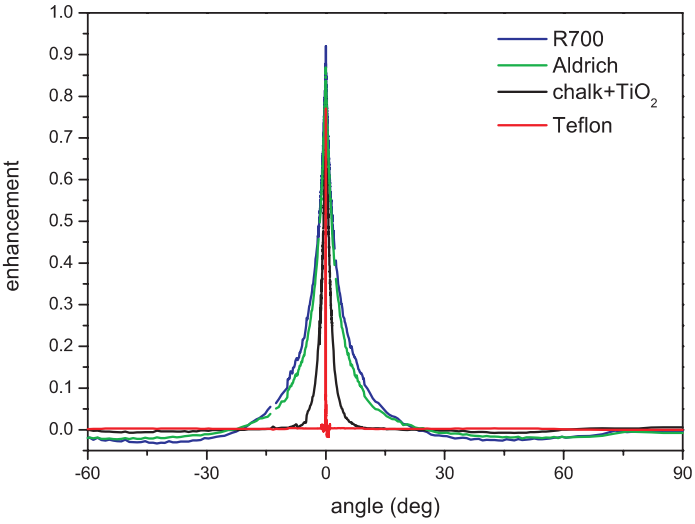

Fig. 2: (Colour on-line) Measurements of backscattering cones for different samples. As the cone width increases, more energy needs to be compensated. Thus the most turbid samples (R700 and Aldrich) lead to a noticeable energy cutback at angles around 45°. The amplitude of this cutback is reduced with decreasing turbidity, but stays positioned around 45°. This indicates that the cutback is due to effects occurring at a fixed length scale close to λ.

an albedo of $A_{\mathrm{ref}} = 0.89$. We thus calculate the ratio of the albedos with respect to the reference and hence the absolute level of the incoherent background for all samples. Subtracting this background then directly gives a proper measure of the backscatter enhancement.

For calibration, the diode signals are measured for the teflon reference at several different incident laser powers, which are determined independently with a calibrated power-meter. Interpolation of the measured data then yields a calibration function for each photodiode [21]. Together with the albedo correction above, this gives an absolute calibration of the intensity for the sample.

Results. – To represent cones with a wide variety of cone widths, we have used samples of ground TiO_2 particles in its rutile structure with different particle diameters (R700: 245 nm and Aldrich: 540 nm), a mixture of TiO_2 (R700) and ground chalk in a weight ratio of one to five, as well as solid teflon. The TiO_2 particles are commercially available as pigment for white paint [15].

As can be seen in figs. 1 and 2, a cutback of the backscattered energy is indeed observed when taking into account the different loss factors of reference and sample. This is most significant for samples with very wide cones like R700 and Aldrich, where the enhancement is noticeably below zero for a range of 50° around ±45°, as shown in fig. 2. The enhancement for teflon is essentially zero away from the cone and in fact gives the intensity resolution of the apparatus, which is of the order of 0.2%. Note that unlike the coherent backscattering peak, the energy cutback is not characterized by a specific

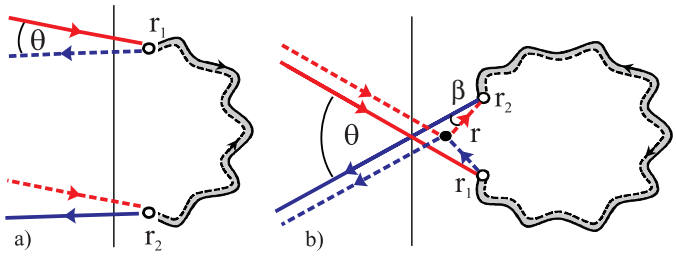

Fig. 3: (Colour on-line) Wave configurations of the contributions H^A and $H^{B,C}$ to coherent backscattering. H^A (a) describes interference between time-reversed amplitudes (full and dashed lines) and gives the classical cone shape [1]. When $\mathbf{r}_1$ and $\mathbf{r}_2$ are within a transverse distance of λ, the time-reversed loops have to be considered as closed and the amplitudes are becoming coupled. This is described by $H^{B,C}$ (b), as an interference effect between the incident plane wave and the attenuated spherical wave traveling between the points $\mathbf{r}_{1,2}$ and a newly introduced scatterer $\mathbf{r}$ at an angle β (see text).

angle but is rather spread out broadly over the whole angular range. Furthermore, these energy cutbacks do compensate the energy enhancements of the cones, as the integral of the enhancement $\alpha(\theta)$ over the backscattering half-space $I = \int \alpha(\theta) \sin\theta \, \mathrm{d}\theta$ is zero for all investigated samples within the margins of error. This shows that a determination of the absolute intensity scale is crucial for the correct observation of the backscattering cone. For such a determination, the different loss factors of reference and sample had to be accounted for.

Theory. – Theoretically, the coherent backscattering cone has been described in great detail [20]. In the geometry of a semi-infinite medium of section S (see fig. 3a), this description makes use of the following well-known expression for the coherent albedo α_c^A:

$$\alpha_c^A = \frac{c}{4\pi S l^{*2}} \int \mathrm{d}\mathbf{r}_1 \, \mathrm{d}\mathbf{r}_2 \, H^A(\mathbf{r}_1, \mathbf{r}_2) \, P(\mathbf{r}_1, \mathbf{r}_2), \qquad (2)$$

where $H^A(\mathbf{r}_1, \mathbf{r}_2) = e^{-\frac{\mu+1}{\mu}\frac{z_1+z_2}{2l^*}} e^{i(\mathbf{k}+\mathbf{k}')\cdot(\mathbf{r}_1-\mathbf{r}_2)}$ for an incident plane wave normal to the interface. $P(\mathbf{r}_1, \mathbf{r}_2)$ is the probability of having a multiple-scattering path starting at $\mathbf{r}_1$ and ending at $\mathbf{r}_2$. The first factor in H^A describes the attenuation of an incident plane wave over a distance of the order of the elastic mean free path l^*. The second factor in H^A accounts for interference and leads to the enhancement with an angular width of order $1/kl^*$. With the scattering vector $q = k \sin\theta$, the evaluation of this integral is well known and yields for the backscattering cone [20]:

$$\alpha_c^A = \frac{3/(8\pi)}{(\frac{\mu+1}{2\mu} + ql^*)^2} \left(\frac{2\mu}{\mu+1} + \frac{1 - \exp(-2\gamma q l^*)}{ql^*} \right). \qquad (3)$$

The interference term H^A is the product of four amplitudes describing the two incoming and the two outgoing plane waves. It is known as a quantum crossing and it is at the origin of coherent effects in quantum mesoscopic physics such as weak localization, universal conductance fluctuations and eventually it leads to the localization transition. Energy (or number of particles) conservation imposes constraints on the quantum crossings. It is well known [19] that in order to fulfill this constraint, two other contributions $H^{B,C}(\mathbf{r}_1, \mathbf{r}_2)$ must be added to H^A, which mix the in- and out-going wave vectors. Energy conservation thus imposes that $\int \mathrm{d}\mathbf{R} \, (H^A + H^B + H^C) = 0$, where $\mathbf{R} = \mathbf{r}_1 - \mathbf{r}_2$.

A complete description of coherent backscattering must therefore include these additional contributions H^B and H^C, which are equal. The physical basis of these contributions lies in a coupling of the light fields at the first and the last scatterer ($\mathbf{r}_1$ and $\mathbf{r}_2$), when they are within a volume of order $\lambda^2 l^*$. This coupling originates in an interference of the incoming plane wave with the multiply scattered spherical wave and is described by introducing an additional scattering event located in $\mathbf{r}$ (see fig. 3b). This is reflected by the short-range behavior of $H^{B,C}(\mathbf{r}_1, \mathbf{r}_2)$ and the additional contribution results from almost closed diffusive trajectories. Consequently, this interference is not restricted to small angles θ as is the case for α_c^A. On the other hand, there is an interesting interference effect between the incoming and outgoing waves. Figure 3b shows that it involves two phase factors of the form $e^{i\mathbf{k}\cdot(\mathbf{r}-\mathbf{r}_1) - ik|\mathbf{r}-\mathbf{r}_1|} = e^{ikR(\cos\beta - 1)}$. The main contribution results from small angles β and the angular integration leaves a very small amplitude, of order $1/kl^*$ for each phase factor. For the case of an incident wave normal to the interface, the contribution α_c^B can be written as

$$\alpha_c^B \simeq \frac{c}{Sl^{*3}} \int \mathrm{d}\mathbf{r} \, P(\mathbf{r}, \mathbf{r}) \, e^{-\frac{\mu+1}{\mu}\frac{z}{l^*}} \, h^2, \qquad (4)$$

where

$$h \simeq -\int \mathrm{d}\mathbf{r}' \, e^{i\mathbf{k}'\cdot\mathbf{r}'} \, \frac{e^{ikr'}}{4\pi r'} \, e^{-r'/2l^*} \simeq \frac{il^*}{2k} \qquad (5)$$

is calculated to leading order in $(kl^*)^{-1}$. It is interesting to note the similarity between h and the shadow term which occurs in the optical theorem and ensures flux conservation for single elastic scattering. Here, the shadow terms h describe the interference between the incident and the multiply scattered waves. The integral in eq. (4) can be solved approximately to give a correction

$$\alpha_c^{B+C} \simeq -\frac{1.15}{(kl^*)^2} \frac{\mu}{\mu+1} \qquad (6)$$

Thus the correction is of order $-(kl^*)^{-2}$. Noting that the angular integral of $\alpha_c^A \simeq (kl^*)^{-2}$, we indeed retrieve the energy conservation condition of quantum crossing, namely that the integral over α_c^{A+B+C} is zero, as it should be.

The expression for α_c^{B+C} shows that the interference effect in eq. (4) is twofold. First, h is purely imaginary so

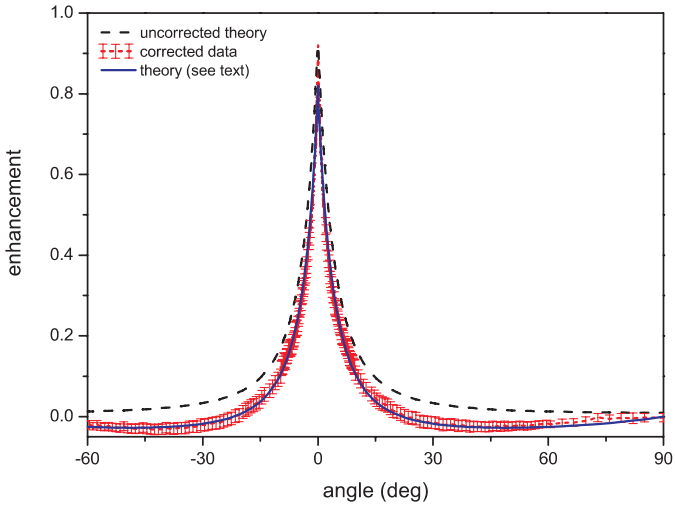

Fig. 4: (Colour on-line) Comparison of the backscattering cone of R700 with corrected and uncorrected enhancement. The agreement between the measured data and the fit of the corrected enhancement α_c^{A+B+C} (dashed) is perfect within the errors. The uncorrected enhancement α_c^{A} (dotted) calculated with the value of kl^* obtained by the fit of the data with α_c^{A+B+C} describes the cone itself quite well, but shows significant deviations in the area of the energy cutback.

that h^2 is negative resulting in a depletion of the coherent albedo proportional to $(kl^*)^{-2}$. Secondly, this interference term does not contribute at a specific angular value but it is rather spread out over the whole angular range.

The scaling of the contribution of the cone with kl^* used here is valid in the diffusion approximation, *i.e.* in the absence of low-order scattering. When low-order scattering is important, a contribution proportional to $(kl^*)^{-1}$ is obtained, which would imply a different correction [23]. In our case however, low-order scattering seems to be negligible as can be seen from the helicity breaking channel shown in fig. 1. In the presence of low-order scattering, a coherent backscattering peak should be observed in the polarization breaking channel as well [12], whereas the small cone observed in the figure is compatible with the measured imperfection of the polarizer foil. Therefore a description in the diffusion approximation as it is carried out above should be sufficient to describe the data.

A fit of the total coherent albedo α_c^{A+B+C} to our data is shown in fig. 4 by the dashed line. The dotted line shows only α_c^{A}, where the same value of kl^* has been used as in α_c^{A+B+C}. Comparing this description with the uncorrected data in fig. 1 shows that the kl^* values determined with those data are close to their real values.

In order to properly determine the turbidity of the sample, the value of kl^* obtained from eq. (3) still has to be corrected for internal reflections [24], which lead to a broader distribution of light paths, and thus to a narrower cone. Furthermore, the ratio between the transport and elastic mean free paths will influence the pre-factor in the correction but is assumed to be close to unity. Carrying out this correction, we find the following values for kl^*: $kl^*_{\mathrm{R700}} = 2.5(2)$, $kl^*_{\mathrm{Ti-Pure}} = 5.0(3)$, $kl^*_{\mathrm{chalk+TiO_2}} = 25(1)$ and $kl^*_{\mathrm{teflon}} = 1950(75)$.

Discussion and conclusions. – We have shown experimentally that coherent backscattering does fulfill conservation of energy. For this purpose, the losses of the reference sample had to be quantified via a time-of-flight measurement to ensure an absolute energy calibration of the setup. If the loss of the reference differs significantly from the loss of the sample, this leads to different positions of the incoherent background in spite of equal incident laser energies.

Furthermore, we have provided a complete theoretical description of coherent backscattering based on the calculation of the three terms $H^{A,B,C}$ that contribute to the Hikami box or quantum crossing. H^A describes the steep angular variation around backscattering and $H^{B,C}$ take into account crossed diagrams dressed by a scattering impurity. Such an impurity provides an additional interference between incoming and multiply scattered waves at short distances. Since the cone is basically the Fourier transform of this intensity this leads to a broadly distributed energy cutback [10]. This improved description of the cone-shape for extremely turbid samples also allows a reliable determination of kl^* in such samples. A comparison of these results with those obtained previously on the same samples shows however that the values of kl^* thus determined change only very little. This implies that the systematic dependence of deviations from classical diffusion is indeed as it was previously determined [14].

* * *

This work was supported by the Deutsche Forschungsgemeinschaft, the International Research and Training Group "Soft Condensed Matter Physics of Model Systems", the Center for Applied Photonics jointly financed by Ministry of Science, Research and Arts of Baden-Württemberg as well as the University of Konstanz, the Israel Academy of Sciences and by the Fund for Promotion of Research at the Technion. Aldrich and DuPont chemicals are acknowledged for providing samples. We also appreciate very much Peter Gross' help in building the backscattering cone setup.

REFERENCES

[1] Akkermans E., Wolf P. E. and Maynard R., *Phys. Rev. Lett.*, **56** (1986) 1471.
[2] Kaveh M., Rosenbluh M., Edrei I. and Freund I., *Phys. Rev. Lett.*, **57** (1986) 2049.
[3] van Albada M. P. and Lagendijk A., *Phys. Rev. Lett.*, **55** (1985) 2692.
[4] Wolf P. E. and Maret G., *Phys. Rev. Lett.*, **55** (1985) 2696.
[5] Kuga Y. and Ishimaru A., *J. Opt. Soc. Am. A*, **1** (1984) 831.

[6] Hapke B. W., Nelson R. M. and Smythe W. D., *Science*, **260** (1993) 509.
[7] Dalichaouch R., Armstrong J. P., Schultz S., Platzman P. M. and McCall S. L., *Nature (London)*, **354** (1991) 53.
[8] Larose E., Margerin L., van Tiggelen B. A. and Campillo M., *Phys. Rev. Lett.*, **93** (2004) 048501.
[9] Bayer G. and Niederdränk T., *Phys. Rev. Lett.*, **70** (1993) 3884.
[10] Akkermans E., Wolf P. E., Maynard R. and Maret G., *J. Phys. (Paris)*, **49** (1988) 77.
[11] van der Mark M. B., van Albada M. P. and Lagendijk A., *Phys. Rev. B*, **37** (1988) 3575.
[12] Lenke R. and Maret G., *Scattering in Polymeric and Colloidal Systems*, edited by Brown W. and Mortensen K. (Gordon and Breach Scientific, New York) 2000, sect. 1.
[13] Anderson P. W., *Phys. Rev.*, **109** (1958) 1492.
[14] Aegerter C. M., Störzer M. and Maret G., *Europhys. Lett.*, **75** (2006) 562.
[15] Störzer M., Gross P., Aegerter C. M. and Maret G., *Phys. Rev. Lett.*, **96** (2006) 063904.
[16] Wiersma D. S., van Albada M. P. and Lagendijk A., *Rev. Sci. Instrum.*, **66** (1995) 5473.
[17] Born M. and Wolf E., *Principles of Optics* (Oxford University Press) 1980.
[18] Dmitriev A. P., Kachorovskii V. Yu. and Gornyi I. V., *Phys. Rev. B*, **56** (1997) 9910.
[19] Hikami S., *Phys. Rev. B*, **24** (1981) 2671.
[20] Akkermans E. and Montambaux G., *Mesoscopic Physics of Electrons and Photons* (Cambridge University Press) 2007.
[21] Gross P., Störzer M., Fiebig S., Clausen M., Maret G. and Aegerter C. M., *Rev. Sci. Instrum.*, **78** (2007) 033105.
[22] Watson G. H., Fleury P. A. and McCall S. L., *Phys. Rev. Lett.*, **58** (1987) 945.
[23] van Tiggelen B. A., Wiersma D. S. and Lagendijk A., *Europhys. Lett.*, **30** (1995) 1.
[24] Zhu J. X., Pine D. J. and Weitz D. A., *Phys. Rev. A*, **44** (1991) 3948.